

Guardians Against Corrosion: Exploring Diphenylpyrazoles Through Experimental and DFT Analysis

A. Mohammed¹, Z. A. Betti², A. F. Hamood³, H. S. Aljibori⁴, W. K. Al-Azzawi⁵, A. A. A. H. Kadhum⁶, A. A. Alamiery^{7,8*}

¹ Department of Electromechanical Engineering, University of Technology-Iraq, P.O. Box: 10001, Baghdad, Iraq

² Technical Engineering College, Middle Technical University, P.O. Box: 10001, Baghdad, Iraq

³ Production and Metallurgy Engineering Department, University of Technology, P.O. Box: 10001, Baghdad, Iraq

⁴ College of Engineering, University of Warith Al-Anbiyaa, P.O. Box: 56001, Karbalaa, Iraq

⁵ Department of Medical Instruments Engineering Techniques, Al-Farahidi University, P.O. Box: 10001, Baghdad, Iraq

⁶ Al-Ameed University College, P. O. Box: 56001, Karbala, Iraq

⁷ Energy and Renewable Energies Technology Center, University of Technology, P.O. Box: 10001, Baghdad, Iraq

⁸ Department of Chemical and Process Engineering, Faculty of Engineering and Build Environment, Universiti Kebangsaan Malaysia, P.O. Box: 43600, Bangi, Selangor, Malaysia.

ARTICLE INFO

Article history:

Received: 16 Jan 2024

Final Revised: 21 Mar 2024

Accepted: 26 Mar 2024

Available online: 30 June 2024

Keywords:

Corrosion

Inhibitor

Adsorption

Isotherm

Physisorption mechanisms

ABSTRACT

This study investigates the potential of 5-amino-1,3-diphenylpyrazole and nitrogen-enriched 5-hydroxy-1,3-diphenylpyrazole to inhibit corrosion of mild steel in acidic environments. A comprehensive approach combining weight loss measurements and Density Functional Theory (DFT) calculations was employed to analyze the inhibitory effect under various concentrations, immersion times, and temperatures. At an optimal concentration of 0.5 mM, 5-amino-1,3-diphenylpyrazole displayed an impressive 94.7% inhibition efficiency, while 5-hydroxy-1,3-diphenylpyrazole achieved 86.4% efficiency at 303 K after 10 hours of exposure. Both compounds exhibited a mixed-type inhibition behavior, with increasing efficiency observed at higher concentrations. DFT calculations provided insights into the interaction between the molecules and the metal surface, along with their electronic properties, aiding in understanding the corrosion inhibition process. The investigation revealed that Langmuir isotherms govern the adsorption mechanism, and the calculated thermodynamic parameters suggest a complex interplay at the metal/solution interface, involving both chemisorption and physisorption. These findings provide valuable knowledge about the mechanisms of corrosion inhibition by these molecules, paving the way for the development of effective strategies to protect mild steel in corrosive environments. Prog. Color Colorants Coat. 18 (2025), 17-35 © Institute for Color Science and Technology.

1. Introduction

Metals, the backbone of our modern world, face a constant adversary - corrosion. This relentless process of degradation silently eats away at their integrity, posing a significant threat to infrastructure, machinery, and overall economic well-being. Imagine bridges

crumbling, pipelines leaking, and industrial equipment failing; the global cost of corrosion paints a grim picture, estimated at a staggering 2.5 trillion dollars annually. This translates to a hefty chunk, roughly 3.4 % of the world's entire economic output [1, 2]. The impact of corrosion extends far beyond mere financial

*Corresponding author: * dr.ahmed1975@ukm.edu.my
dr.ahmed1975@gmail.com

<https://doi.org/10.30509/pccc.2024.167261.1276>

implications. Its insidious nature jeopardizes the safety and functionality of critical structures across various industries [3]. Pipelines transporting essential resources like oil and gas become susceptible to breaches, bridges supporting heavy traffic risk structural failure, and industrial equipment vital for manufacturing processes experiences malfunctions. These consequences not only disrupt daily life but also pose environmental hazards and hinder economic progress [4-7]. Among the environments that accelerate corrosion, acidic solutions present a particularly daunting challenge. Imagine the harsh conditions within industrial settings where processes often involve the use of strong acids like hydrochloric acid (HCl). These acidic environments wreak havoc on metal surfaces, necessitating the development of effective strategies to combat this destructive force [8, 9]. The scientific community has embarked on a relentless pursuit of solutions to mitigate corrosion. One promising approach involves the utilization of corrosion inhibitors. These specialized chemicals act like shields, forming a protective layer on the metal surface, thereby hindering the aggressive attack by corrosive agents [10]. Researchers have explored various types of corrosion inhibitors, with organic compounds emerging as a particularly promising class. These molecules, often characterized by the presence of nitrogen, oxygen, or sulfur atoms, possess the unique ability to bond with metal surfaces, offering effective protection. Additionally, the inherent versatility of organic chemistry allows for the tailoring of these molecules' structures for specific applications [11, 12]. This study delves into the potential of two specific organic compounds, 5-amino-1,3-diphenylpyrazole and 5-hydroxy-1,3-diphenylpyrazole, as potential corrosion inhibitors for mild steel in acidic environments. The presence of nitrogen atoms in their structures piques scientific interest, as these atoms are known to play a crucial role in the inhibition process.

To gain a comprehensive understanding of how these molecules inhibit corrosion, the study adopts a two-pronged approach. First is experimental techniques, which represent a well-established method called weight loss measurement, will be employed to assess the effectiveness of the inhibitors under varying conditions, including concentration, immersion time, and temperature. This approach provides valuable real-world insights into the inhibitors' performance [13, 14]. Second, Density Functional Theory (DFT) calculations will be utilized to delve deeper into the world of atoms

and molecules. This powerful computational tool sheds light on the interactions between the inhibitors and the metal surface, along with their electronic properties and adsorption behavior. By simulating these interactions at the microscopic level, DFT offers valuable insights into the underlying mechanisms governing the inhibition process [15].

This combined approach is crucial for not only evaluating the effectiveness of the chosen inhibitors but also for unraveling the intricate dance between these molecules and the metal surface. Understanding the fundamental mechanisms that govern the inhibition process is essential for the rational design of even more potent corrosion inhibitors in the future [16, 17]. The knowledge gained from this research is expected to contribute significantly to the development of robust and long-lasting protection strategies for mild steel in acidic environments. By understanding the science behind corrosion inhibition at a fundamental level, the study aims to pave the way for the design of more effective and targeted solutions, ultimately fostering the development of a more sustainable and corrosion-resistant future for our infrastructure and machinery. This study embarks on a detailed investigation into the potential of 5-amino-1,3-diphenylpyrazole and 5-hydroxy-1,3-diphenylpyrazole (Figure 1) to combat corrosion in mild steel exposed to acidic environments. These molecules, particularly intriguing due to the presence of nitrogen atoms, hold promise as effective corrosion inhibitors.

The inhibitory mechanisms of 5-amino-1,3-diphenylpyrazole and 5-hydroxy-1,3-diphenylpyrazole against mild steel corrosion in acidic environments were thoroughly explored through weight loss techniques and Density Functional Theory (DFT) analysis. Complementing these methods, Scanning Electron Microscopy (SEM) was employed to investigate the inhibitors' effects on mild steel in HCl solution. In the existing body of literature, multiple studies underscore the effectiveness of

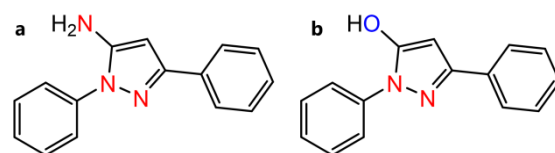


Figure 1: Chemical structures of the investigated molecules: (a) 5-amino-1,3-diphenylpyrazole and (b) 5-hydroxy-1,3-diphenylpyrazole.

corrosion inhibitors, particularly those containing nitrogen, oxygen, π -bonds, resonance effects, and heteroatoms, in combating HCl-induced corrosion of mild steel. It is widely acknowledged that inhibitors possessing a combination of these elements exhibit superior inhibitory performance compared to those with only one of them. The prevailing assumption is that the adsorption mechanism primarily involves the nitrogen and oxygen atoms within the synthesized pyrazoles [18].

Numerous scholarly works emphasize the significance of organic corrosion inhibitors featuring electron donor atoms such as phosphorus, sulfur, oxygen, and nitrogen for surface adsorption on metals, thereby safeguarding against acidic solutions. Among these heteroatoms, nitrogen demonstrates notable inhibitive efficacy, followed by phosphorus, sulfur, and oxygen. Natural plant extracts have attracted interest due to their excellent qualities, which include affordability, renewable nature, biodegradability, and environmental friendliness. However, organic inhibitors may encounter challenges related to limited solubility in polar electrolytes due to their inherent hydrophobic nature [19]. Typically, organic corrosion inhibitors comprise nitrogen, hydrophobic hydrocarbon chains, sulfur, and oxygen moieties in their molecular structures. The effectiveness of these inhibitors hinges on various factors, such as molecular size, aromaticity, bonding atoms or groups (π or σ), charge distribution, and electronic structure. Computational chemistry techniques like DFT have proven invaluable in elucidating the inhibitory properties of organic compounds [20].

The inhibitory efficiency of 5-amino-1,3-diphenylpyrazole and 5-hydroxy-1,3-diphenylpyrazole was compared with other nitrogen-containing corrosion inhibitors for safeguarding mild steel against corrosion. For instance, a corrosion inhibitor, namely 7-((1-(4-fluorobenzyl)-1H-1,2,3-triazol-4-yl)methyl)-1,3-dimethyl-3,7-dihydro-1H-purine-2,6-dione [21], exhibited an inhibition efficiency of 86 %. However, this compound exhibited lower efficiency compared to 5-amino-1,3-diphenylpyrazole. Similarly, corrosion inhibitors like 3,5-di(m-tolyl)-4-amino-1,2,4-triazole, 3-salicylidene amino-1,2,4-triazole phosphonate, 3-benzylidene amino-1,2,4-triazole phosphonate, 3-p-nitro-benzylidene amino-1,2,4-triazole phosphonate, and 1-amino-3-methyl thio-1,2,4-triazole [22, 23], despite containing a triazole ring and amino group, exhibited much lower inhibition efficiencies (24, 63, 56, 69, and 43 %, respectively) compared to the studied inhibitors. Another study

investigated the use of 3,5-bis(methylene octadecyl-dimethylammonium chloride)-1,2,4-triazole [24] as a corrosion inhibitor. Although it demonstrated high inhibition efficiency (98 %), its high cost rendered it less favorable. In contrast, 5-amino-3-mercapto-1,2,4-triazole, while easy to synthesize and stable, exhibited an inhibition efficiency of 90 % [25], slightly lower than that of the studied inhibitor. 5-amino-1,3-diphenylpyrazole displayed superior inhibitory efficiency compared to the aforementioned compounds and exhibited efficiency levels comparable to those described in [21-25]. Moreover, as the concentration of 5-amino-1,3-diphenylpyrazole increased, the corrosion rate decreased, indicating an enhancement in inhibitive efficacy, possibly attributable to increased adsorption of the inhibitor on the mild steel surface with increasing concentration.

2. Experimental

2.1. Corrosive environment

A 1 M hydrochloric acid (HCl) solution was prepared for this study. Analytical reagent-grade HCl (37 %) was diluted with double-distilled water to achieve the desired concentration.

2.2. Weight loss measurements

Experiments were conducted in a 1 M HCl solution, with and without the presence of the inhibitors: 5-amino-1,3-diphenylpyrazole and 5-hydroxy-1,3-diphenylpyrazole. Mild steel coupons were prepared as detailed in Table 1. These coupons were $45 \times 25 \times 0.2$ mm in size and underwent thorough sanding using various grades of sandpaper, reaching a final grade of 1200. Each experiment utilized a 250 mL beaker containing 100 mL of the 1 M HCl solution [26, 27].

Table 1: Chemical composition of the tested mild steel coupons.

Element	Composition (%)
Carbon	0.210
Manganese	0.050
Silicon	0.380
Aluminum	0.010
Sulfur	0.050
Phosphorus	0.090
Iron	Balance

The pre-cleaned coupons were meticulously weighed before being submerged in the 1 M HCl solution. Exposure times varied from 1 to 120 hours, with experiments conducted in both the absence and presence of the inhibitors (5-amino-1,3-diphenylpyrazole and 5-hydroxy-1,3-diphenylpyrazole) at different concentrations ranging from 0.1 to 1 mM. After each exposure period, the coupons were retrieved from the solution, rinsed thoroughly with double-distilled water to remove any residual acid. Next, they were washed with acetone to eliminate any organic contaminants. Following a drying process in an oven, the coupons were weighed again using a high-precision electronic balance. The corrosion rate (in millimeters per year) and the protection efficiency (%) were calculated using the weight loss data obtained and established equations (equations 1 and 2) [28].

$$\text{Corrosion Rate (mm/year)} = 87.6 \times \frac{\Delta W}{a \times t} \quad (1)$$

$$\text{IE\%} = 1 - \frac{W_i - W_f}{W_i} \times 100 \quad (2)$$

equations 1 and 2 [28] are used to calculate the corrosion rate and this value, expressed in millimeters per year (mm/year), indicates the rate at which the metal deteriorates due to corrosion, and also protection efficiency (%) parameter, and this parameter reflects the effectiveness of the inhibitors in hindering the corrosion process.

Variables in the Equations:

- ΔW : Represents the weight loss of the coupon during the experiment (in grams).
- A : Denotes the surface area of the coupon (in square centimeters).
- t : Represents the exposure time of the coupon to the corrosive solution (in hours).
- W_i : Represents the initial weight of the coupon before exposure (in grams).
- W_f : Represents the final weight of the coupon after exposure (in grams).

2.3. Effect of temperature

The influence of temperature on the corrosion process was investigated at four different temperatures: 303, 313, 323, and 333 K. Coupons with dimensions of $45 \times 25 \times 0.2$ mm were used in each test. The experiment setup involved a 250 mL beaker containing 100 mL of 1 M HCl solution as the corrosive medium. Similar to the previous section, clean coupons were weighed,

immersed for 5 hours, and retrieved from the solution. This process was carried out in the absence and presence of the inhibitors at varying concentrations (0.1 to 1 mM) at each temperature. After exposure, the standard cleaning procedure (rinsing, washing, drying, and reweighing) was followed. To ensure accuracy, each weight loss experiment was repeated three times [29, 30].

2.4. Adsorption isotherms and understanding inhibitor-metal interactions

Understanding the chemical interactions of organic inhibitors with metal surfaces requires an analysis of adsorption isotherms. This section explores the adsorption behavior of the chosen inhibitors (5-amino-1,3-diphenylpyrazole and 5-hydroxy-1,3-diphenylpyrazole) on mild steel in a 1 M HCl environment. The investigation involves analyzing the relationship between the corrosion rate and the extent to which the inhibitor covers the metal surface (represented by θ , the reciprocal of inhibition efficiency). This analysis is performed by fitting the data into various mathematical models (Langmuir, Frumkin, Temkin, Freundlich, and Flory-Huggins) expressed in linear form (equations 3-7).

$$\frac{C_R}{\theta} = \frac{1}{K_{ads}} + C_R \quad (3)$$

$$\log \left[C_R \left(\frac{\theta}{1-\theta} \right) \right] = 2\alpha\theta + 2.393 \log K_{ads} \quad (4)$$

$$\theta = \ln C_R + K_{ads} \quad (5)$$

$$\log \theta = n \log C_R + \log K_{ads} \quad (6)$$

$$\log \frac{\theta}{C_R} = b \log (1 - \theta) + \log K_{ads} \quad (7)$$

Where:

- Degree of Surface Coverage (θ): This value indicates the extent to which the inhibitor molecules occupy the metal surface.
- Corrosion Rate (C): This parameter reflects the rate at which the metal deteriorates due to corrosion.
- Equilibrium Adsorption Constant (K_{ads}): This constant quantifies the strength of the interaction between the inhibitor and the metal surface.

The benefits of adsorption isotherms are that analyzing the data obtained through these models allows researchers to gain a deeper understanding of the inhibitor-metal surface interaction, and by

determining the adsorption constants and the maximum coverage values, scientists can obtain quantitative information crucial for designing more effective corrosion inhibitors.

2.5. Scanning electron microscopy (SEM)

A TM1000 Hitachi Tabletop Microscope was used to perform SEM analysis on mild steel samples. These samples were immersed in a 1 M HCl solution for 3 hours at 303 K, both in the absence and presence of the corrosion inhibitors at a concentration of 0.5 mM. This technique allows for the visualization of the microstructures and surface morphologies of the samples, providing insights into the inhibitor's influence on the metal surface.

2.6. Computational details

Software called Gaussian 03 was used to determine the optimized molecular structures (ground-state geometries) of the investigated molecules. A specific set of mathematical functions (6-31G++(d,p)) was employed to describe the electronic structure of the atoms within the molecules. The B3LYP functional, a combination of two established methods, was utilized to calculate various properties like the Highest Occupied Molecular Orbital (HOMO), energy the Lowest Unoccupied Molecular Orbital (LUMO) energy and additional physical properties. Specific equations 8-12 were used to calculate several parameters, including HOMO, LUMO, energy gap (ΔE), electronic negativity (η), electronegativity difference (σ), absolute electronegativity (χ), and charge transfer (ΔN) [31, 32].

$$\Delta E = E_{LUMO} - E_{HOMO} \quad (8)$$

$$\eta = -\frac{1}{2}(E_{LUMO} - E_{HOMO}) \quad (9)$$

$$\sigma = \frac{1}{\eta} \quad (10)$$

$$\chi = -\frac{1}{2}(E_{LUMO} + E_{HOMO}) \quad (11)$$

$$\Delta N = \frac{\chi_{Fe} - \chi_{inh}}{2(\eta_{Fe} + \eta_{inh})} \quad (12)$$

Electronegativity reflects an atom's ability to attract electrons toward itself in a chemical bond. The absolute electronegativity values of the metal and inhibitor are denoted by symbols χ_{Fe} and χ_{inh} , respectively. Hardness refers to a material's resistance to permanent shape changes from external pressure.

The absolute hardness values of the metal and inhibitor are represented by symbols η_{Fe} and η_{inh} , respectively.

The charge transfer (ΔN) parameter quantifies the movement of electrons between the metal and the inhibitor molecule during the adsorption process. In the case of iron (Fe), the equation for ΔN can be expressed as equation 13 ($\chi_{Fe} = 7$ eV and $\eta_{Fe} = 0$).

$$\Delta N = \frac{7 - \chi_{inh}}{2\eta_{inh}} \quad (13)$$

3. Results and Discussion

3.1. Effect of inhibitor concentrations

The influence of inhibitor concentration on the corrosion rate of mild steel in 1 M HCl solution was investigated at various temperatures (303, 313, 323, and 333 K) using 5-amino-1,3-diphenylpyrazole and 5-hydroxy-1,3-diphenylpyrazole. Figure 2 a and b showcases the effectiveness of these inhibitors. As the concentration increases at 303 K, the inhibition efficiency rises significantly. Without any inhibitors (0 mM concentration), the corrosion rate of mild steel was 4.31 mm/year. At an optimal concentration of 0.5 mM, 5-amino-1,3-diphenylpyrazole considerably reduced the corrosion rate to 0.31 mm/year at 303 K [33, 34]. A similar trend was observed with 5-hydroxy-1,3-diphenylpyrazole, achieving a corrosion rate of 0.36 mm/year at its optimal concentration. This concentration-dependent decrease in weight loss highlights the effectiveness of both inhibitors in protecting mild steel from corrosion in hydrochloric acid. The experiment confirms that both inhibitors hinder corrosion. As the concentration increases, the corrosion rate decreases, and the inhibition efficiency improves [35, 36]. Notably, at 0.5 mM concentration and after a 10-hour exposure, 5-amino-1,3-diphenylpyrazole and 5-hydroxy-1,3-diphenylpyrazole achieved impressive inhibition efficiencies of 94.7% and 86.4%, respectively. The presence of nitrogen atoms in 5-amino-1,3-diphenylpyrazole and the combination of oxygen and nitrogen atoms in 5-hydroxy-1,3-diphenylpyrazole likely contribute to their inhibitory properties. These elements facilitate a strong interaction with the mild steel surface. Furthermore, these compounds' intrinsic stability and resonance effect increase how efficient they are at inhibiting corrosion.

Both inhibitors effectively reduce corrosion, but 5-amino-1,3-diphenylpyrazole shows slightly better

performance across various concentrations and temperatures. This difference might be due to the unique interactions between the inhibitor molecules and the metal surface, influenced by their distinct chemical structures.

3.2. Effect of exposure time

The impact of immersion time on corrosion behavior was studied using weight loss measurements. Figure 3 shows the results for various exposure durations (1, 5, 10, 24, 48, and 120 hours) in the presence of both inhibitors. Corrosion rates decrease with increasing inhibitor concentration and exposure time, indicating a time-dependent effect [38, 39]. At a concentration of 0.1 mM, both inhibitors show a significant decrease in corrosion rate after 10 hours compared to 1 hour, highlighting the progressive protection with time.

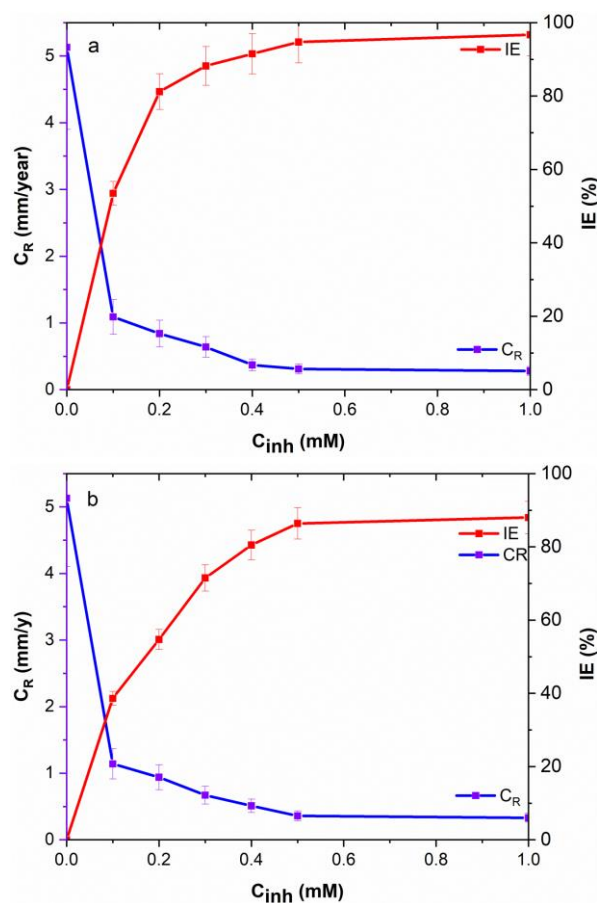


Figure 2: The variation of corrosion rate (CR) and inhibition efficiency (IE %) with different concentrations of (a) 5-amino-1,3-diphenylpyrazole and (b) 5-hydroxy-1,3-diphenylpyrazole and the experiment was conducted for 5 hours at 303 K on mild steel immersed in 1 M HCl solution.

Inhibition efficiencies follow a similar trend, increasing with longer exposure durations [40]. At the optimal concentration of 0.5 mM, both inhibitors exhibit impressive inhibition efficiencies after 10 hours, demonstrating their sustained effectiveness. Notably, the efficiencies remain stable after 24 hours, suggesting a potential saturation point in the inhibitory action. This plateau effect indicates that extending exposure time beyond a certain point might not significantly improve inhibition. The observed stability after 24 hours is crucial for practical applications, suggesting a consistent and optimized inhibitor-metal interaction. Understanding this equilibrium state is important for optimizing inhibitor usage and making informed decisions about exposure times in real-world scenarios [41].

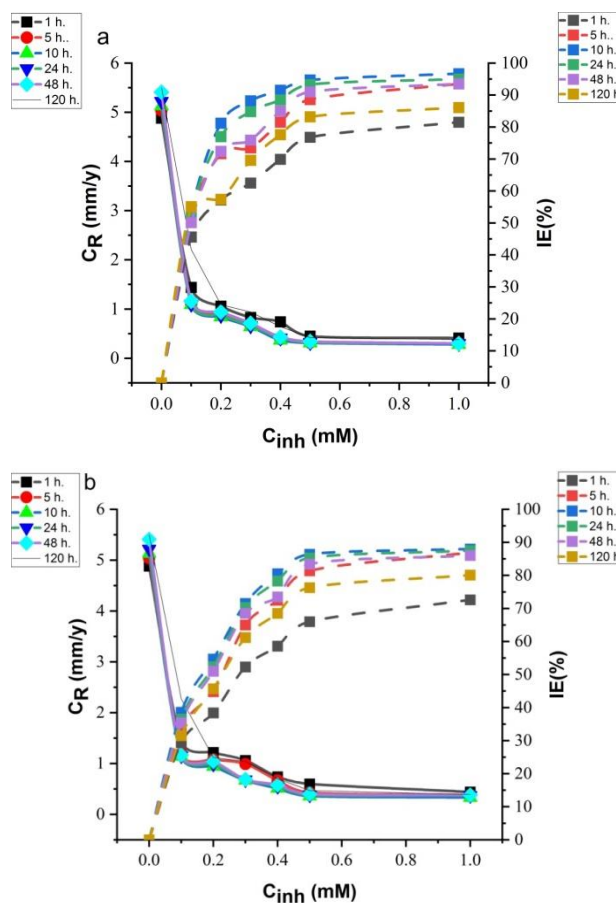


Figure 3: Corrosion rates and inhibition efficiencies of mild steel exposed to (a) 5-amino-1,3-diphenylpyrazole and (b) 5-hydroxy-1,3-diphenylpyrazole at different concentrations and exposure times in 1 M HCl solution.

Figure 4 explores the performance of both inhibitors over a longer exposure time (120 hours) to assess their effectiveness in long-term corrosion prevention. At a concentration of 0.1 mM, both inhibitors show a slight decrease in inhibition efficiency with extended exposure. This effect becomes more prominent at the optimal concentration (0.5 mM). After 120 hours, the inhibition efficiency of 5-amino-1,3-diphenylpyrazole drops from its initial value to 83 %. Similarly, 5-hydroxy-1,3-diphenylpyrazole shows a decrease to 71 % efficiency after 120 hours. Even after extended exposure, both inhibitors continue to show significant efficacy in reducing corrosion, although the noted decline.

While both inhibitors remain effective after extended exposure (120 hours), their inhibition efficiency slightly weakens. This suggests potential limitations for long-term use. Factors like inhibitor depletion, environmental changes, or film alterations might contribute to this decrease. Despite the decrease, these inhibitors show promise for real-world scenarios requiring long-term protection, such as pipelines or structures in harsh environments. Further studies are needed to understand the mechanisms behind the efficiency decrease over longer durations.

3.3. Temporal trends, practical implications, and comparative analysis

Studies reveal that the effectiveness of both inhibitors (5-amino-1,3-diphenylpyrazole and 5-hydroxy-1,3-diphenylpyrazole) changes over time. As exposure time increases, their ability to hinder corrosion (inhibition

efficiency) improves. This suggests the formation of a protective layer on the metal surface, gradually slowing down the corrosion process [42, 43]. This time-dependent behavior is particularly relevant for situations requiring long-term corrosion protection, such as pipelines, industrial equipment, and structures exposed to harsh environments. Comparing the two inhibitors, 5-amino-1,3-diphenylpyrazole generally shows slightly better performance at various exposure durations. Based on exposure conditions, this comparison aids in selecting the best inhibitor for a certain application [44, 45]. The chosen range (1 to 120 hours) allows researchers to firstly examine both short-term and long-term corrosion behaviors; this time frame captures the initial stages of corrosion and potential changes in corrosion rates over time and secondly; this duration is feasible for setting up experiments, collecting data, and ensuring efficient research within a reasonable timeframe. Many industrial and environmental settings involve exposure to corrosive agents for varying durations (hours to days). Studying corrosion within this range provides insights applicable to real-world situations, like the corrosion of building materials. This time frame enables comparison with previous studies in corrosion inhibition, facilitating the identification of trends and potential variations in corrosion behavior under similar conditions. Selecting exposure times from 1 to 120 hours offers a comprehensive understanding of corrosion behavior and the effectiveness of inhibitors over different durations [46, 47].

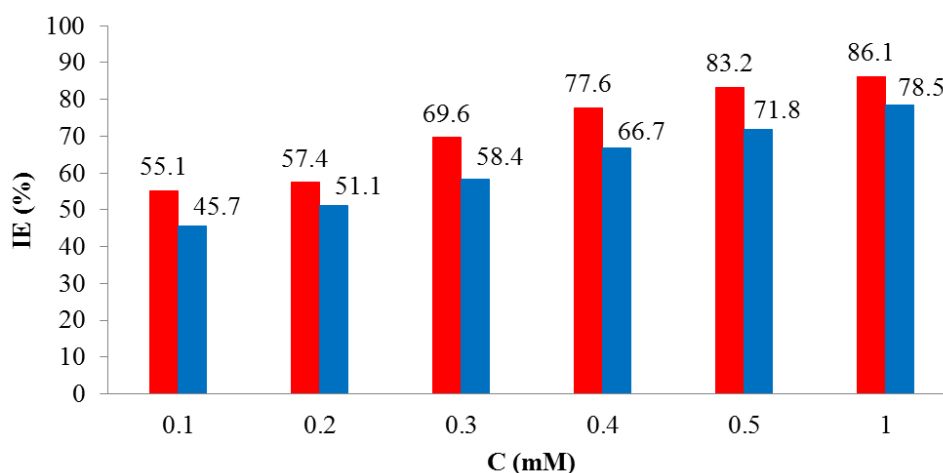


Figure 4: Inhibition efficiencies of mild steel exposed to (red color) 5-amino-1,3-diphenylpyrazole and (red color) 5-hydroxy-1,3-diphenylpyrazole at different concentrations and 120 hour as exposure times in 1 M HCl solution.

3.4. Effect of temperature

Figure 5 explores how temperature impacts the corrosion-inhibiting properties of 5-amino-1,3-diphenylpyrazole and 5-hydroxy-1,3-diphenylpyrazole. Different temperatures (303, 313, 323, and 333 K) were tested in a 1 M HCl solution to gain insights into the "thermal behavior" of these inhibitors. As expected, corrosion rates steadily increase with rising temperature. This aligns with the established principle that higher temperatures intensify corrosive processes. Interestingly, despite the rising corrosion rates, both inhibitors exhibit remarkable stability in their inhibition efficiencies across all temperatures. This resilience signifies their consistent inhibitory action, even under challenging conditions of elevated temperatures. The stability of inhibition efficiency with temperature suggests that the protective layer formed by the inhibitors on the metal surface is thermally stable. These layer likely functions by creating a physical barrier between the metal and the corrosive environment. This temperature resilience makes these inhibitors suitable for real-world applications where temperature fluctuations are unavoidable [48, 49]. This is particularly relevant in industries like:

- Chemical processing: Reactors and pipelines often operate at elevated temperatures.
- Power generation: Boilers and heat exchangers experience significant temperature variations.
- Oil and gas exploration: Pipelines and equipment encounter varying temperatures throughout their lifecycle.

While both inhibitors demonstrate stability, further investigations are necessary to understand the underlying mechanisms responsible for their temperature resistance. This could involve analyzing the composition and structure of the protective layer formed at different temperatures and, investigating the interaction between the inhibitor molecules and the metal surface under varying thermal conditions. The ability to maintain substantial inhibition efficiency at elevated temperatures positions these inhibitors as promising candidates for corrosion prevention in diverse industrial settings. Their robustness offers reliable solutions for various practical applications.

3.5. Langmuir adsorption isotherm analysis: unraveling the molecular interaction

The Langmuir adsorption isotherm is a helpful tool for

studying how inhibitor molecules interact with metal surfaces. This analysis provides insights into how effectively the inhibitors (5-amino-1,3-diphenylpyrazole and 5-hydroxy-1,3-diphenylpyrazole) bind to the mild steel surface [50]. The analysis using the Langmuir isotherm confirms that both inhibitors effectively adsorb onto the mild steel surface, forming a protective layer that hinders corrosion. This finding aligns with the observed decrease in corrosion rates with increasing inhibitor concentrations.

3.5.1. 5-Amino-1,3-diphenylpyrazole: deciphering adsorption dynamics

The Langmuir adsorption isotherm for 5-amino-1,3-diphenylpyrazole (Figure 6a) is expressed by the equation $y = 0.06234 + 0.95944x$, where 'y' represents the inhibition efficiency and 'x' denotes the inhibitor concentration.

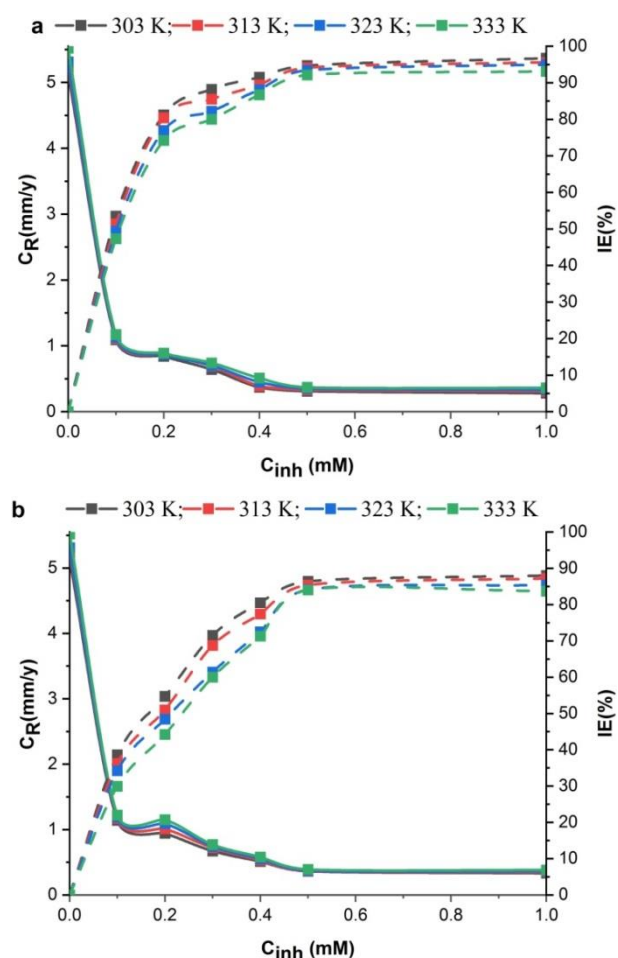


Figure 5: Corrosion rate and inhibition efficiency dynamics under varied temperature and inhibitor concentrations for (a) 5-amino-1,3-diphenylpyrazole and (b) 5-hydroxy-1,3-diphenylpyrazole.

The statistical parameters reveal a high degree of correlation ($R\text{-Square} = 0.99699$), indicating the robustness of the Langmuir model in explaining the adsorption behavior. The positive slope (0.95944) suggests a direct proportionality between the inhibitor concentration and inhibition efficiency, reinforcing the monolayer adsorption mechanism proposed by the Langmuir model. The intercept (0.06234) provides insights into the efficiency at lower concentrations, showcasing that even at minimal inhibitor concentrations; there is a notable inhibitory effect. The data suggests a strong correlation between inhibitor concentration and its effectiveness in preventing corrosion (Figure 6a). As the concentration increases, the inhibition efficiency rises steadily. This indicates that more inhibitor molecules are attaching to the metal surface, forming a protective layer. Even at low concentrations, the inhibitor demonstrates a noticeable ability to reduce corrosion, highlighting its potential for practical applications.

3.5.2. 5-Hydroxy-1,3-diphenylpyrazole: Unveiling adsorption characteristics

For 5-hydroxy-1,3-diphenylpyrazole, the Langmuir adsorption isotherm (Figure 6b) is represented by the equation $y = 0.13893 + 0.96908x$. The statistical parameters exhibit a strong correlation ($R\text{-Square} = 0.98879$), affirming the applicability of the Langmuir model to describe the adsorption process. The positive slope (0.96908) signifies a direct relationship between the inhibitor concentration and inhibition efficiency, consistent with monolayer adsorption behavior. The intercept (0.13893) indicates a notable inhibitory effect even at lower concentrations, supporting the Langmuir model's assertion of monolayer coverage at the metal surface. Similar to the first inhibitor, this molecule also exhibits a direct relationship between concentration and inhibition efficiency (Figure 6b). The data supports the idea that the inhibitor forms a single layer (monolayer) on the metal surface, effectively hindering corrosion. Like the previous inhibitor, even low concentrations show a positive impact on corrosion prevention.

The analysis confirms that the chosen model (the Langmuir isotherm) effectively describes how these inhibitors interact with the metal surface. As the inhibitor concentration increases, its effectiveness in preventing corrosion (inhibition efficiency) also increases. This suggests that more inhibitor molecules

are attaching to the metal surface, potentially forming a single layer (monolayer). Even at low concentrations, both inhibitors show a positive impact on corrosion prevention, highlighting their potential for practical applications. An important factor is the stability of the inhibitor layer on the metal surface. This is determined by a property called "standard Gibbs free energy of adsorption." In this study, the calculated values for both inhibitors were negative, indicating that the adsorption process is spontaneous and the formed layer is stable. The calculated values in this study fall between the ranges for both physical and chemical adsorption, suggesting a combined mechanism might be at play [51-53].

The calculated ΔG_{ads}^0 values in this study (-33.22 kJ/mol for 5-amino-1,3-diphenylpyrazole and -35.49 kJ/mol for 5-hydroxy-1,3-diphenylpyrazole) align with the characteristics of both physical adsorption and chemisorption processes.

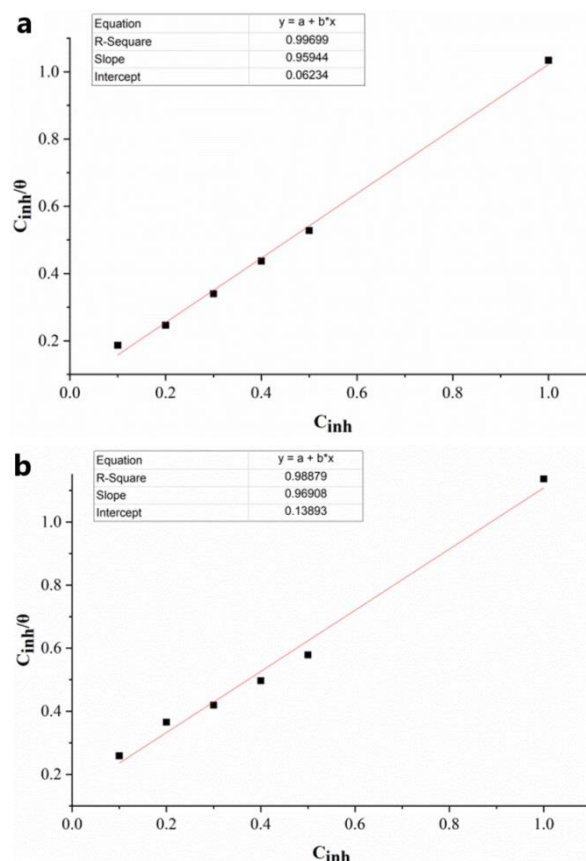


Figure 6: Langmuir adsorption isotherm analysis for (a) 5-amino-1,3-diphenylpyrazole and (b) 5-hydroxy-1,3-diphenylpyrazole.

The standard Gibbs free energy of adsorption (ΔG_{ads}^0) is determined by the equation 14:

$$\Delta G_{ads}^0 = -RT \ln(55.5 K_{ads}) \quad (14)$$

Where:

- R is the gas constant (8.314 J/(mol·K)),
- T is the absolute temperature (298 K),
- K_{ads} is the equilibrium adsorption constant.

The negative values of ΔG_{ads}^0 affirm the effectiveness of 5-amino-1,3-diphenylpyrazole and 5-hydroxy-1,3-diphenylpyrazole as corrosion inhibitors in 1 M HCl solution, highlighting their ability to form stable adsorbed layers on the mild steel surface.

3.6. SEM investigations

Scanning electron microscopes (SEM) provide high-resolution images of the metal surface, allowing us to directly observe the effects of the inhibitors. The surface untreated sample (Figure 7a) appears rough and damaged, with signs of corrosion products. This confirms the aggressive nature of the acidic environment. In contrast, samples treated with inhibitors as in Figures 7b and 7c show significantly smoother surfaces with fewer signs of damage. This indicates the formation of a protective layer by the inhibitors. Combining the findings from the Langmuir isotherm analysis and SEM observations, it's evident that both inhibitors effectively form a stable layer on the metal surface, shielding it from the corrosive effects of the acidic environment.

3.7. DFT theoretical chemical calculations

In this study, the application of Density Functional Theory (DFT) provides valuable insights into the electronic structure of the inhibitors, 5-amino-1,3-diphenylpyrazole and 5-hydroxy-1,3-diphenylpyrazole. The HOMO and LUMO energy levels, along with various calculated parameters, shed light on the electronic characteristics influencing the inhibition efficiencies. The HOMO-LUMO energy gap (ΔE) is a crucial parameter indicating the stability of a molecule [54, 55]. The calculated parameters (Table 2) contribute to the understanding of inhibitor-metal surface interactions. A smaller HOMO-LUMO gap (ΔE)

indicates higher stability, while global hardness (η) and softness (σ) reflect the ability of the inhibitor to donate or accept electrons. The electronegativity (χ) signifies the tendency to attract electrons. Inhibitors with appropriate values of these parameters tend to exhibit enhanced inhibition efficiencies. The calculated ΔN values suggest that both inhibitors possess characteristics favorable for effective adsorption, contributing to their corrosion inhibition properties. The combination of DFT calculations and experimental data provides a comprehensive insight into the mechanisms governing the inhibitory action of these compounds [56, 57].

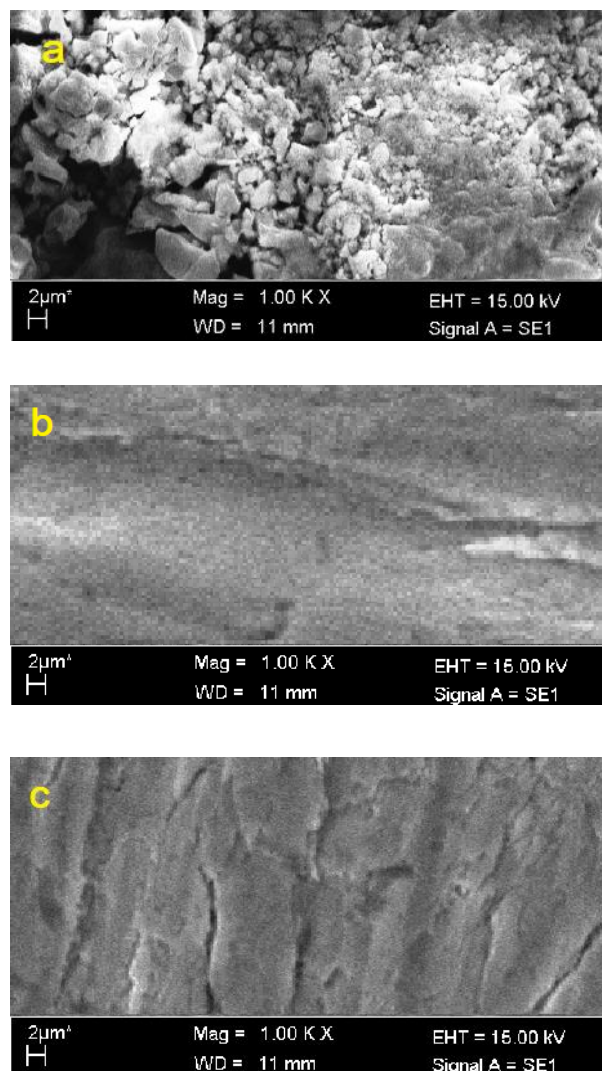


Figure 7: SEM of mild steel (a) without and with (b) 5-amino-1,3-diphenylpyrazole and (c) 5-hydroxy-1,3-diphenylpyrazole at 0.5 mM concentrations and 3 h as exposure time in 1 M HCl solution.

Table 2: The quantum chemical parameters.

Parameter	Discussion	5-Amino-1,3-diphenylpyrazole	5-Hydroxy-1,3-diphenylpyrazole
ΔE	Both inhibitors exhibit similar energy gaps, indicating comparable reactivity towards the metal surface.	-6.792 eV	-6.899 eV
η	The negative values suggest both inhibitors tend to accept electrons, influencing their inhibitory capabilities.	- 3.396 eV	-3.449 eV
σ	The small magnitude implies both inhibitors are relatively soft, responding more readily to changes in electron density.	-0.2949 eV ⁻¹	-0.2900 eV ⁻¹
χ	Both inhibitors possess similar values, reflecting their ability to donate electrons to the metal surface.	4.935 eV	4.513 eV
ΔN	The positive values suggest a tendency to withdraw electrons, aligning with their electron-accepting nature.	0.3036	0.3035

The quantum parameters derived from DFT calculations offer a detailed insight into the electronic features of 5-amino-1,3-diphenylpyrazole and 5-hydroxy-1,3-diphenylpyrazole. While both inhibitors share similarities in several aspects, the subtle variations in these parameters play a crucial role in shaping their distinctive inhibitory behaviors. The discussion below elucidates the implications of these quantum parameters and their potential contributions to the corrosion inhibition mechanisms of the two compounds. In conclusion, the nuanced differences in these quantum parameters play a pivotal role in shaping the inhibitory behaviors of 5-amino-1,3-diphenylpyrazole and 5-hydroxy-1,3-diphenylpyrazole. These electronic characteristics provide valuable insights into the potential mechanisms through which the inhibitors interact with the metal surface and mitigate corrosion. The electron-accepting nature, adaptability to changes in electron density, and the ability to donate electrons collectively contribute to the inhibitory efficacy of these compounds, emphasizing their promising roles in corrosion inhibition strategies [58, 59].

The analysis of the electrophilic and nucleophilic reactive sites, represented by the LUMO and HOMO, respectively, reveals key insights into the corrosion inhibition mechanisms of 5-amino-1,3-diphenylpyrazole and 5-hydroxy-1,3-diphenylpyrazole, as illustrated in Figure 8. In the case of 5-amino-1,3-diphenylpyrazole, the nucleophilic site (HOMO) extends across the three Nitrogen atoms, while the electrophilic reactive site (LUMO) covers the entire molecule and the terminal phenyl ring (Figure 8). This configuration implies that 5-amino-1,3-diphenylpyrazole can potentially initiate attacks from all nitrogen atoms. The higher electron-releasing tendency compared to the electron-accepting tendency is a key factor contributing to the robust adsorption of 5-amino-1,3-diphenylpyrazole. The

elevated E_{HOMO} value and a small ΔE further support significant inhibitor adsorption on mild steel (Table 2). The terminal carbon atoms, phenyl rings, and/or the heterocyclic ring accept electrons donated by mild steel, while nitrogen atoms in 5-amino-1,3-diphenylpyrazole also contribute to the electron donation [60, 61]. Consequently, a strong physiochemisorption mechanism is anticipated for 5-amino-1,3-diphenylpyrazole, facilitated by back donation of electrons. In contrast, the nucleophilic site (HOMO) for 5-hydroxy-1,3-diphenylpyrazole extends over one oxygen and two nitrogen atoms, while the electrophilic reactive site (LUMO) encompasses the entire molecule and the terminal phenyl ring (Figure 8). The reactive sites suggest potential attacks from both Nitrogen and Oxygen atoms. Similar to 5-amino-1,3-diphenylpyrazole, the higher electron-releasing tendency compared to the electron-accepting tendency is a prominent factor driving the strong adsorption of 5-hydroxy-1,3-diphenylpyrazole. The elevated E_{HOMO} value and a small ΔE further enhance the adsorption potential on mild steel (Table 2). The terminal carbon atoms, phenyl rings, and/or the heterocyclic ring accept electrons from mild steel, while both oxygen and nitrogen atoms in 5-hydroxy-1,3-diphenylpyrazole contribute to electron donation. This configuration supports a strong physiochemisorption mechanism for 5-hydroxy-1,3-diphenylpyrazole, facilitated by the back donation of electrons [62, 63].

In summary, the distinctive electronic configurations of 5-amino-1,3-diphenylpyrazole and 5-hydroxy-1,3-diphenylpyrazole, characterized by their reactive sites, contribute to their respective corrosion inhibition mechanisms. The analysis underscores the significance of electron-donating tendencies and back donation processes, providing a comprehensive understanding of the inhibitors' interactions with the mild steel surface and their inhibitory efficacy.

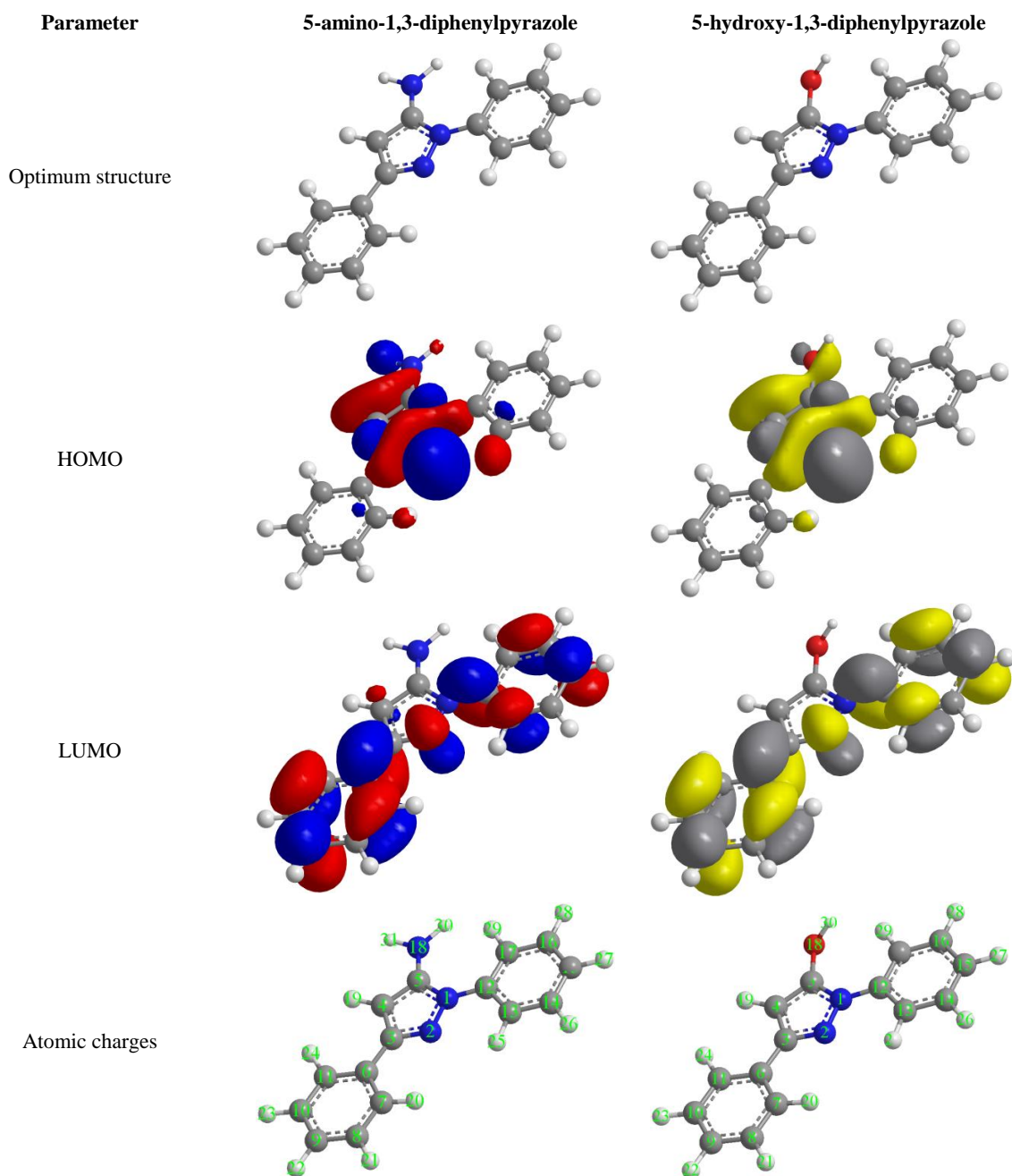


Figure 8: The optimized structures, HOMO, LUMO and atomic numberd structures of 5-amino-1,3-diphenylpyrazole and 5-hydroxy-1,3-diphenylpyrazole

The atomic charges of 5-amino-1,3-diphenylpyrazole and 5-hydroxy-1,3-diphenylpyrazole, as presented in Table 3, provide valuable insights into the potential interactions between these inhibitors and the mild steel surface [64, 65]. For both inhibitors, the nitrogen atoms (N) play a crucial role. In 5-amino-1,3-diphenylpyrazole, nitrogen atoms in the pyrrole (N(1)) and imine (N(2)) moieties exhibit charge characteristics suggesting potential interactions with the mild steel surface. Similarly, in 5-hydroxy-1,3-diphenylpyrazole, the

Nitrogen atom in the pyrrole (N(1)) exhibits a positive charge, indicating its potential to interact with the metal. The Carbon atoms (C) in the alkene moieties contribute to the electron density and may participate in bonding interactions with the mild steel surface. The charges on Carbon atoms (C(3) to C(17)) are relatively small, indicating a limited role in electron donation or acceptance. In 5-hydroxy-1,3-diphenylpyrazole, the oxygen atom (O(18)) in the enol group exhibits a negative charge, suggesting a propensity to donate

electrons. This suggests that the Oxygen atom can contribute to the interaction with the mild steel surface [66, 67]. These atomic charges, when considered in conjunction with the molecular structure, provide valuable information about the potential bonding sites and the nature of interactions between the inhibitors and the mild steel surface. Further investigation into the interplay of these charged sites with the d-orbitals of iron would be essential to comprehend the detailed mechanism of corrosion inhibition [68, 69].

3.8. Suggested inhibition mechanism

3.8.1. Inhibition mechanism of 5-amino-1,3-diphenylpyrazole

1- Adsorption on mild steel surface: 5-amino-1,3-diphenylpyrazole possesses nucleophilic sites (nitrogen atoms in pyrrole and imine moieties), which can interact with the positively charged mild steel surface.

The adsorption involves the formation of a protective layer on the metal surface [70-73].

2- Electron donor characteristics: The electron-releasing tendency of 5-amino-1,3-diphenylpyrazole, indicated by its high HOMO energy level, facilitates the donation of electrons to the mild steel surface. This electron transfer contributes to the stability of the adsorbed layer [74, 75].

3- Physiochemisorption mechanism: The combination of electron donation from the inhibitor and acceptance by the mild steel surface supports a strong physiochemisorption mechanism. Back donation of electrons from nitrogen atoms enhances the stability of the adsorbed layer, providing effective corrosion inhibition [76].

4- Charge interaction: The charged nature of the nitrogen atoms allows for electrostatic interactions with the charged metal surface, contributing to inhibition efficiency.

Table 3: Atomic charges for 5-amino-1,3-diphenylpyrazole and 5-hydroxy-1,3-diphenylpyrazole.

Atom	Atom type	Atomic charges	
		5-amino-1,3-diphenylpyrazole	5-hydroxy-1,3-diphenylpyrazole
N(1)	N Pyrrole	0	0.685242
N(2)	N Imine	0.636436	-0.331546
C(3)	C Alkene	0.0272879	0.031006
C(4)	C Alkene	-0.464133	-0.337014
C(5)	C Alkene	0.184914	0.208273
C(6)	C Alkene	0.0416443	0.0478966
C(7)	C Alkene	-0.0666749	-0.0644955
C(8)	C Alkene	-0.0272197	-0.0254114
C(9)	C Alkene	-0.0703824	-0.0634197
C(10)	C Alkene	-0.0246587	-0.024612
C(11)	C Alkene	-0.0743275	-0.0684331
C(12)	C Alkene	0.133794	0.146102
C(13)	C Alkene	-0.110868	-0.0903398
C(14)	C Alkene	-0.0269073	-0.0258969
C(15)	C Alkene	-0.104867	-0.0806918
C(16)	C Alkene	-0.0260079	-0.0246195
C(17)	C Alkene	-0.123766	-0.0989896
N(18)	N Enamine	0.033202	—
O(18)	O Enol	—	-0.330383

3.8.2. Inhibition mechanism of 5-hydroxy-1,3-diphenylpyrazole

1- Adsorption on mild steel surface: 5-Hydroxy-1,3-diphenylpyrazole, with nucleophilic sites (nitrogen and oxygen atoms), can absorb onto the mild steel surface. The adsorption process involves the formation of a protective layer that impedes the corrosion process [77].

2- Electron donor characteristics: Similar to 5-amino-1,3-diphenylpyrazole, 5-hydroxy-1,3-diphenylpyrazole exhibits electron-releasing tendencies, particularly from nitrogen and oxygen atoms. This electron donation enhances the interaction with the metal surface.

3- Physiochemisorption mechanism: The electron donation from the inhibitor and acceptance by the mild steel surface supports a physiochemisorption mechanism. The back donation of electrons from Nitrogen and Oxygen atoms contributes to the stability of the adsorbed layer.

4- Charge interaction: The charged nature of nitrogen and oxygen atoms allows for electrostatic interactions with the charged metal surface, contributing to the inhibition efficiency.

To comprehend the intricate impact of 5-amino-1,3-diphenylpyrazole and 5-hydroxy-1,3-diphenylpyrazole on the mild steel surface in the presence of 1 M HCl, a comprehensive examination is crucial. This involves a thorough analysis of the test outcomes and their correlation with the chemical, electronic, and structural attributes of the inhibitor particles. Both 5-amino-1,3-diphenylpyrazole and 5-hydroxy-1,3-diphenylpyrazole are rich in heteroatoms, rendering them as Lewis bases.

These molecules form coordination bonds with the free d-orbitals of iron and adsorb onto the mild steel surface. This adsorption process results in the creation of a protective layer, acting as a shield against corrosive media. Consequently, the interaction between inhibitor particles and iron surfaces can be intricately mediated by a combination of chemisorption and physisorption processes. Furthermore, the involvement of retro-donation, utilizing electronic pi-electrons, further contributes to the stability of the adsorbed layer [78, 79]. The proposed mechanism for the mild steel surface adsorption strategy by 5-amino-1,3-diphenylpyrazole and 5-hydroxy-1,3-diphenylpyrazole is depicted in Figure 9. This visual representation captures the multifaceted nature of the adsorption process, showcasing the formation of protective layers through coordination bonds, electrostatic interactions, and retro-donation mechanisms. The robust inhibitory effect of these compounds on mild steel corrosion is a testament to the sophisticated interplay of their chemical and electronic properties, establishing them as promising corrosion inhibitors in acidic environments.

In summary, both inhibitors operate through a combination of adsorption, electron donation, and physiochemisorption mechanisms. The specific characteristics of each inhibitor, such as the presence of nitrogen and oxygen atoms and their electron-donating tendencies, play a crucial role in forming a protective layer on the mild steel surface and inhibiting corrosion. The charged nature of these atoms facilitates strong interactions with the metal surface, contributing to the effectiveness of the inhibitors.

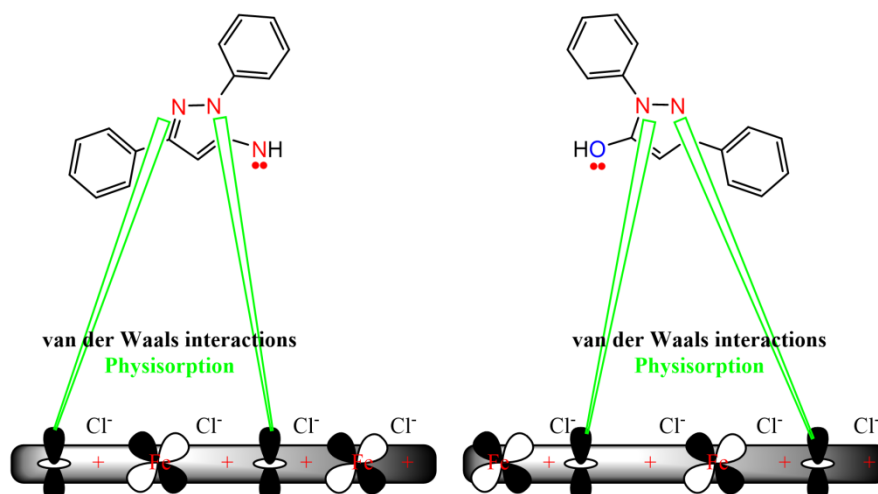


Figure 9: Suggested inhibition mechanism of adsorption behaviour of 5-amino-1,3-diphenylpyrazole and 5-hydroxy-1,3-diphenylpyrazole on mild steel surface.

4. Conclusion

In conclusion, this research has provided valuable insights into the corrosion inhibition potential of 5-amino-1,3-diphenylpyrazole and 5-hydroxy-1,3-diphenylpyrazole for mild steel in acidic media. Through a meticulous experimental and theoretical approach, the inhibitory performance of these compounds was systematically evaluated, shedding light on their effectiveness under varying conditions. The experimental findings, particularly the weight loss measurements, revealed a notable increase in inhibition efficiency with escalating inhibitor concentrations. Both 5-amino-1,3-diphenylpyrazole and 5-hydroxy-1,3-diphenylpyrazole exhibited remarkable inhibition efficiencies, reaching up to 94.7 and 86.4 %, respectively, at optimal concentrations. The concentration-dependent decrease in corrosion rate underscored the inhibitory effect of these compounds, showcasing their potential as corrosion inhibitors in hydrochloric acid. The exploration of exposure time and temperature effects further emphasized the sustained effectiveness of the inhibitors. Notably, the inhibitory efficiency remained impressive even with prolonged exposure, signifying the durability of the protective layers formed on the mild steel surface. Additionally, the inhibitors demonstrated resilience to temperature variations, highlighting their potential application in diverse environmental conditions. The integration of DFT calculations and adsorption isotherm

studies enriched the understanding of the inhibitory mechanism. The Langmuir adsorption isotherm model aptly described the adsorption behavior, emphasizing the formation of protective layers through chemisorption and physisorption processes. The calculated standard Gibbs free energy of adsorption values confirmed the spontaneity and stability of the adsorption process, positioning these inhibitors as promising candidates for mild steel corrosion protection. Furthermore, the theoretical insights gained from DFT calculations, including quantum parameters and electronic properties, provided a comprehensive overview of the inhibitors' electronic characteristics. The correlation of these parameters with inhibition efficiencies offered a nuanced understanding of the inhibitory behavior, paving the way for the design and development of more effective corrosion inhibitors. In summary, the combination of experimental measurements, theoretical calculations, and in-depth analyses has elucidated the inhibitory potential of 5-amino-1,3-diphenylpyrazole and 5-hydroxy-1,3-diphenylpyrazole. These compounds exhibit multifaceted inhibitory mechanisms, making them promising candidates for mitigating mild steel corrosion in acidic environments. This research contributes not only to the field of corrosion science but also offers a foundation for the rational design of novel and efficient corrosion inhibitors for diverse industrial applications.

5. References

1. Mahdi BS, Abbass MK, Mohsin MK, Al-Azzawi WK, Hanoon MM, Al-Kaabi MH, Shaker LM, Al-Amiery AA, Isahak WN, Kadhum AA, Takriff MS. Corrosion inhibition of mild steel in hydrochloric acid environment using terephthaldehyde based on Schiff base: Gravimetric, thermodynamic, and computational studies. *Molecules*. 2022; 27(15):4857. <https://doi.org/10.3390/molecules27154857>.
2. A. Jawad Q, S. Zinad D, DawoodSalim R, A Al-Amiery A, Sumer Gaaz T, Takriff MS, H. Kadhum AA. Synthesis, characterization, and corrosion inhibition potential of novel thiosemicarbazone on mild steel in sulfuric acid environment. *Coatings*. 2019; 9(11):729. <https://doi.org/10.3390/coatings9110729>.
3. Al-Baghdadi SB, Noori FT, Ahmed WK, Al-Amiery AA. Thiadiazole as a potential corrosion inhibitor for mild steel in 1 M HCl. *J Adv Electrochem*. 2016; 18:67-9.
4. Resen AM, Hanoon M, Salim RD, Al-Amiery AA, Shaker LM, Kadhum AA. Gravimetric, theoretical, and surface morphological investigations of corrosion inhibition effect of 4-(benzimidazole-2-yl) pyridine on mild steel in hydrochloric acid. *KOM Corr Mater Protect J*. 2020; 64(4):122-30. <https://doi.org/10.2478/kom-2020-0018>.
5. Junaedi S, Al-Amiery AA, Kadhum A, Kadhum AA, Mohamad AB. Inhibition effects of a synthesized novel 4-aminoantipyrine derivative on the corrosion of mild steel in hydrochloric acid solution together with quantum chemical studies. *Inter J Mol Sci*. 2013; 14(6):11915-28. <https://doi.org/10.3390/ijms140611915>.
6. Solomon MM, Uzoma IE, Olugbuyiro JA, Ademosun OT. A censorious appraisal of the oil well acidizing corrosion inhibitors. *J Petrol Sci Eng*. 2022; 215:110711. <https://doi.org/10.1016/j.petrol.2022.110711>.

7. Alamri AH. Localized corrosion and mitigation approach of steel materials used in oil and gas pipelines—An overview. *Eng Fail Anal.* 2020; 116:104735. <https://doi.org/10.1016/j.engfailanal.2020.104735>.
8. Alamiery AA, Isahak WN, Aljibori HS, Al-Asadi HA, Kadhum AA. Effect of the structure, immersion time and temperature on the corrosion inhibition of 4-pyrrol-1-yl-n-(2, 5-dimethyl-pyrrol-1-yl) benzoylamine in 1.0 M HCl solution. *Inter J Corr Scale Inhib.* 2021; 10(2):700-13. <https://doi.org/10.17675/2305-6894-2021-10-2-14>.
9. Al-Azzawi WK, Al Adily AJ, Sayyid FF, Al-Azzawi RK, Kzar MH, Jawoosh HN, Al-Amiery AA, Kadhum AA, Isahak WN, Takriff MS. Evaluation of corrosion inhibition characteristics of an N-propionanilide derivative for mild steel in 1 M HCl: Gravimetric and computational studies. *Int J Corro Scale Inhib.* 2022; 11(3):1100-14. <https://doi.org/10.17675/2305-6894-2022-11-3-12>.
10. Khudhair AK, Mustafa AM, Hanoon MM, Al-Amiery A, Shaker LM, Gazz T, Mohamad AB, Kadhum AH, Takriff MS. Experimental and theoretical investigation on the corrosion inhibitor potential of N-MEH for mild steel in HCl. *Prog Color Colorant Coat.* 2022; 15(2):111-22. <https://doi.org/10.30509/PCCC.2021.166815.1111>.
11. Mustafa AM, Sayyid FF, Betti N, Hanoon MM, Al-Amiery A, Kadhum AA, Takriff MS. Inhibition evaluation of 5-(4-(1H-pyrrol-1-yl) phenyl)-2-mercapto-1,3,4-oxadiazole for the corrosion of mild steel in an acidic environment: thermodynamic and DFT aspects. *Tribologia-Finnish J Tribol.* 2021; 38(3-4):39-47. <https://doi.org/10.30678/fjt.105330>.
12. Al-Baghdadi SB, Hashim FG, Salam AQ, Abed TK, Gaaz TS, Al-Amiery AA, Kadhum AA, Reda KS, Ahmed WK. Synthesis and corrosion inhibition application of NATN on mild steel surface in acidic media complemented with DFT studies. *Results Phys.* 2018; 8:1178-84. <https://doi.org/10.1016/j.rinp.2018.02.007>.
13. Abdulsahib YM, Eltmimi AJ, Alhabeeb SA, Hanoon MM, Al-Amiery AA, Allami T, Kadhum AA. Experimental and theoretical investigations on the inhibition efficiency of N-(2, 4-dihydroxy-tolueneylidene)-4-methylpyridin-2-amine for the corrosion of mild steel in hydrochloric acid. *Inter J Corr Scale Inhib.* 2021; 10(3):885-99. <https://doi.org/10.17675/2305-6894-2021-10-3-3>.
14. Zinad DS, Salim RD, Betti N, Shaker LM, Al-Amiery AA. Comparative investigations of the corrosion inhibition efficiency of a 1-phenyl-2-(1-phenylethylidene) hydrazine and its analog against mild steel corrosion in hydrochloric acid solution. *Prog Color Colorant Coat.* 2022; 15(1):53-63. <https://doi.org/10.30509/pccc.2021.166786.1108>.
15. Salim RD, Betti N, Hanoon M, Al-Amiery AA. 2-(2, 4-Dimethoxybenzylidene)-N-phenylhydrazinecarbothioamide as an efficient corrosion inhibitor for mild steel in acidic environment. *Progr Color Colorant Coat.* 2022; 15(1):45-52. <https://doi.org/10.30509/pccc.2021.166775.1105>.
16. Al-Amiery AA, Shaker LM, Kadhum AH, Takriff MS. Exploration of furan derivative for application as corrosion inhibitor for mild steel in hydrochloric acid solution: Effect of immersion time and temperature on efficiency. *Mater Today: Proc.* 2021; 42:2968-73. <https://doi.org/10.1016/j.matpr.2020.12.807>.
17. Resen AM, Hanoon MM, Alani WK, Kadhim A, Mohammed AA, Gaaz TS, Kadhum AA, Al-Amiery AA, Takriff MS. Exploration of 8-piperazine-1-ylmethylumbelliferone for application as a corrosion inhibitor for mild steel in hydrochloric acid solution. *Inter J Corr Scale Inhib.* 2021; 10(1):368-87. <https://doi.org/10.17675/2305-6894-2021-10-1-21>.
18. Alamiery A. Corrosion inhibition effect of 2-N-phenylamino-5-(3-phenyl-3-oxo-1-propyl)-1, 3, 4-oxadiazole on mild steel in 1 M hydrochloric acid medium: Insight from gravimetric and DFT investigations. *Mater Sci Energy Technol.* 2021; 4:398-406. <https://doi.org/10.1016/j.mset.2021.09.002>.
19. Al-Amiery, A.A., Mohamad, A.B., Kadhum, A.A.H. *et al.* Experimental and theoretical study on the corrosion inhibition of mild steel by nonanedioic acid derivative in hydrochloric acid solution. *Sci Rep.* 2022; 12: 4705. <https://doi.org/10.1038/s41598-022-08146-8>.
20. Yang HM. Role of organic and eco-friendly inhibitors on the corrosion mitigation of steel in acidic environments—a state-of-art review. *Molecules.* 2021; 26(11):3473. <https://doi.org/10.3390/molecules26113473>.
21. Vyshnevskaya Yu P, Brazhnyk IV. Corrosion prevention and control using in situ phase layers formation via application of the complexing-type inhibitors. *Appl. Res.* 2023. <https://doi.org/10.1002/appl.202300027>.
22. Espinoza-Vázquez A, Rodríguez-Gómez FJ, Martínez-Cruz IK, Ángeles-Beltrán D, Negrón-Silva GE, Palomar-Pardavé M, Romero LL, Pérez-Martínez D, Navarrete-López AM. Adsorption and corrosion inhibition behaviour of new theophylline-triazole-based derivatives for steel in acidic medium. *R Soc Open Sci.* 2019; 6(3):181738.
23. Hassan HH, Abdelghani E, Amin MA. Inhibition of mild steel corrosion in hydrochloric acid solution by triazole derivatives: Part I. Polarization and EIS studies. *Electrochimica Acta.* 2007; 52(22): 6359-6366.
24. Ramesh S, Rajeswari S. Corrosion inhibition of mild steel in neutral aqueous solution by new triazole derivatives. *Electrochim Acta.* 2004; 49(5): 811-820. <https://doi.org/10.1016/j.electacta.2003.09.035>.
25. Qiu LG, Xie AJ, Shen YH. A novel triazole-based cationic gemini surfactant: synthesis and effect on corrosion inhibition of carbon steel in hydrochloric

- acid. *Mater Chem Phys*. 2005; 91(2-3):269-273. <https://doi.org/10.1016/j.matchemphys.2004.11.022>.
26. Abdulazeez MS, Abdullahe ZS, Dawood MA, Handel ZK, Mahmood RI, Osamah S, Kadhum AH, Shaker LM, Al-Amiery AA. Corrosion inhibition of low carbon steel in HCl medium using a thiadiazole derivative: weight loss, DFT studies and antibacterial studies. *Int J Corr Scale Inhib*. 2021; 10(4):1812-28. <https://doi.org/10.17675/2305-6894-2021-10-4-27>
 27. Mahmood D, Al-Okbi AK, Hanon MM, Rida KS, Alkaim AF, Al-Amiery AA, Kadhum A, Kadhum AA. Carbethoxythiazole corrosion inhibitor: as an experimentally model and DFT theory. *J Eng Appl Sci*. 2018; 13(11):3952. <https://doi.org/10.3923/JEASCI.2018.3952.3959>.
 28. ASTM International, Standard Practice for Preparing, Cleaning, and Evaluating Corrosion Test, 2011, 1–9.
 29. NACE International, Laboratory Corrosion Testing of Metals in Static Chemical Cleaning Solutions at Temperatures below 93°C (200°F), TM0193-2016-SG, 2000.
 30. Alamiery A, Mahmoudi E, Allami T. Corrosion inhibition of low-carbon steel in hydrochloric acid environment using a Schiff base derived from pyrrole: gravimetric and computational studies. *Inter J Corr Scale Inhib*. 2021; 10(2):749-65. <https://doi.org/10.17675/2305-6894-2021-10-2-17>
 31. Gaussian09 RA. 1, mjfrisch, gw trucks, hbschlegel, gescuseria, ma robb, jrcheeseman, g. Scalmani, v. Barone, b. Mennucci, gapetersson et al., gaussian. Inc., Wallingford CT. 2009; 121:150-66.
 32. Manamela KM, Murulana LC, Kabanda MM, Ebenso EE. Adsorptive and DFT studies of some imidazolium based ionic liquids as corrosion inhibitors for zinc in acidic medium. *Inter J Electrochem Sci*. 2014; 9(6):3029-46.
 33. Koopmans T. Ordering of wave functions and eigenenergies to the individual electrons of an atom. *Physica*. 1933; 1:104-13. [https://doi.org/10.1016/S0031-8914\(34\)90011-2](https://doi.org/10.1016/S0031-8914(34)90011-2).
 34. Eltmimi AJ, Alamiery A, Allami AJ, Yusop RM, Kadhum AH, Allami T. Inhibitive effects of a novel efficient Schiff base on mild steel in hydrochloric acid environment. *Inter J Corr Scale Inhib*. 2021; 10(2):634-48. <https://doi.org/10.17675/2305-6894-2021-10-2-10>.
 35. Singh AK, Pandey AK, Banerjee P, Saha SK, Chugh B, Thakur S, Pani B, Chaubey P, Singh G. Eco-friendly disposal of expired anti-tuberculosis drug isoniazid and its role in the protection of metal. *J Environ Chem Eng*. 2019; 7(2):102971. <https://doi.org/10.1016/j.jece.2019.102971>.
 36. Benabdellah M, Tounsi A, Khaled KF, Hammouti B. Thermodynamic, chemical and electrochemical investigations of 2-mercapto benzimidazole as corrosion inhibitor for mild steel in hydrochloric acid solutions. *Arabian J Chem*. 2011; 4(1):17-24. <https://doi.org/10.1016/j.arabjc.2010.06.010>.
 37. Dawood MA, Alasady ZM, Abdulazeez MS, Ahmed DS, Sulaiman GM, Kadhum AA, Shaker LM, Alamiery AA. The corrosion inhibition effect of a pyridine derivative for low carbon steel in 1 M HCl medium: Complemented with antibacterial studies. *Int J Corr Scale Inhib*. 2021; 10(4):1766-82. <https://doi.org/10.17675/2305-6894-2021-10-4-25>.
 38. Alamiery AA. Anticorrosion effect of thiosemicarbazide derivative on mild steel in 1 M hydrochloric acid and 0.5 M sulfuric Acid: Gravimetric and theoretical studies. *Mater Sci Energy Technol*. 2021; 4:263-73. <https://doi.org/10.1016/j.mset.2021.07.004>.
 39. Alamiery AA, Isahak WN, Aljibori HS, Al-Asadi HA, Kadhum AA. Effect of the structure, immersion time and temperature on the corrosion inhibition of 4-pyrrol-1-yl-n-(2, 5-dimethyl-pyrrol-1-yl) benzoyl-amine in 1.0 m HCl solution. *Inter J Corr Scale Inhib*. 2021; 10(2):700-13. <https://doi.org/10.17675/2305>.
 40. Haldhar R, Prasad D, Saxena A, Singh P. Valerianawallichii root extract as a green & sustainable corrosion inhibitor for mild steel in acidic environments: experimental and theoretical study. *Mater Chem Front*. 2018; 2(6):1225-37. <https://doi.org/10.1039/C8QM00120K>.
 41. Singh AK, Shukla SK, Ebenso EE. Cefacetrile as corrosion inhibitor for mild steel in acidic media. *Inter J Electrochem Sci*. 2011; 6(11):5689-700.
 42. Al-Bghdadi SB, Hanoon MM, Odah JF, Shaker LM, Al-Amiery AA. Benzylidene as efficient corrosion inhibition of mild steel in acidic solution. *Multidisciplinary Digital Publishing Institute Proceedings*. 2019; 41(1):27. <https://doi.org/10.3390/ecsoc-23-06472>.
 43. Mahdi BS, Aljibori HS, Abbass MK, Al-Azzawi WK, Kadhum AH, Hanoon MM, Isahak WN, Al-Amiery AA, Majdi HS. Gravimetric analysis and quantum chemical assessment of 4-aminoantipyrine derivatives as corrosion inhibitors. *Int J Corr Scale Inhib*. 2022; 11(3):1191-213. <https://doi.org/10.17675/2305-6894-2022-11-3-17>.
 44. Alamiery AA. Study of corrosion behavior of N'-(2-(2-oxomethylpyrrol-1-yl) ethyl) piperidine for mild steel in the acid environment. *Biointerface Res Appl Chem* 2022; 12(3):3638-46. <https://doi.org/10.33263/BRIAC123.36383646>.
 45. Sharma SK, Peter A, Obot IB. Potential of Azadirachta indica as a green corrosion inhibitor against mild steel, aluminum, and tin: a review. *J Anal Sci Technol*. 2015; 6(1):1-6. <https://doi.org/10.1186/s40543-015-0067-0>.
 46. Adejo SO, Yias SG, Leke L, Onuche M, Atondo MV, Uzah TT. Corrosion studies of mild steel in sulphuric acid medium by acidimetric method. *Inter J Corr Scale Inhib*. 2019; 8(1):50-61.
 47. Adejo SO. Proposing a new empirical adsorption isotherm known as Adejo-Ekwenchi isotherm. *J Appl Chem*. 2014; 6(5):66-71. <https://doi.org/10.9790/5736-0656671>.

48. Siaka AA, Eddy NO, Idris SO, Mohammed A, Elinge CM, Atiku FA. FTIR spectroscopic information on the corrosion inhibition potentials of ampicillin in HCl solution. *Innov Sci Eng*. 2012;2 :41-8.
49. Al-Senani GM. Corrosion inhibition of carbon steel in acidic chloride medium by Cucumissativus (cucumber) peel extract. *Int J Electrochem Sci*. 2016; 11(1):291-302.
50. Langmuir I. The constitution and fundamental properties of solids and liquids. II. Liquids. *J Am Chem Soc*. 1917; 39(9):1848-906. <https://doi.org/10.1021/ja02254a006>.
51. Ho YS, Porter JF, McKay G. Equilibrium isotherm studies for the sorption of divalent metal ions onto peat: copper, nickel and lead single component systems. *Water Air Soil Poll*. 2002; 141:1-33.
52. Popova A, Christov M, Vasilev A, Zvetanova A. Mono- and dicationic benzothiazolic quaternary ammonium bromides as mild steel corrosion inhibitors. Part I: Gravimetric and voltammetric results. *Corr Sci*. 2011; 53(2):679-86.
53. Mohammed A, Aljibori HS, Al-Hamid MAI, Al-Azzawi WK, Kadhum AAH, Alamiery A. N-Phenyl-N'-[5-phenyl-1,2,4-thiadiazol-3-yl]thiourea: corrosion inhibition of mild steel in 1 M HCl. *Int J Corros Scale Inhib*. 2024; 13(1):38-78. <https://doi.org/10.17675/2305-6894-2024-13-1-3>.
54. Vorobyova V, Overchenko T, Skiba M. Experimental and theoretical investigations of anti-corrosive properties of thymol. *Chem Chem Techno*. 2019; 13(2): 261-268. <https://doi.org/10.23939/chcht13.02.261>.
55. Sastri VS, Perumareddi JR. Molecular orbital theoretical studies of some organic corrosion inhibitors. *Corrosion*. 1997; 53(8): 33-48. <https://doi.org/10.5006/1.3290294>.
56. Benali O, Larabi L, Traisnel M, Gengembre L, Harek Y. Electrochemical, theoretical and XPS studies of 2-mercapto-1-methylimidazole adsorption on carbon steel in 1 M HClO₄. *Appl Surf Sci*. 2007; 253(14):6130-9. <https://doi.org/10.1016/j.apsusc.2007.01.075>.
57. Khaled KF, Al-Qahtani MM. The inhibitive effect of some tetrazole derivatives towards Al corrosion in acid solution: Chemical, electrochemical and theoretical studies. *Mater Chem Phys*. 2009; 113(1):150-8. <https://doi.org/10.1016/j.matchemphys.2008.07.060>.
58. Hmamou DB, Salghi R, Zarrouk A, Zarrok H, Touzani R, Hammouti B, El Assyry A. Investigation of corrosion inhibition of carbon steel in 0.5 M H₂SO₄ by new bipyrazole derivative using experimental and theoretical approaches. *J Environ Chem Eng*. 2015; 3(3):2031-41. <https://doi.org/10.1016/j.jece.2015.03.018>.
59. Ma H, Chen S, Liu Z, Sun Y. Theoretical elucidation on the inhibition mechanism of pyridine-pyrazole compound: a HartreeFock study. *J Mol Struct*. 2006; 774(1-3):19-22. <https://doi.org/10.1016/j.theochem.2006.06.044>.
60. Mourya P, Singh P, Tewari AK, Rastogi RB, Singh MM. Relationship between structure and inhibition behaviour of quinolinium salts for mild steel corrosion: experimental and theoretical approach. *Corr Sci*. 2015; 95:71-87. <https://doi.org/10.1016/j.corsci.2015.02.034>.
61. Stern M, Geary AL. Electrochemical polarization: I. A theoretical analysis of the shape of polarization curves. *J Electrochem Soc*. 1957; 104(1):56. <https://doi.org/10.1149/1.2428496>.
62. Olanakanmi LO, Obot IB, Kabanda MM, Ebenso EE. Some quinoxalin-6-yl derivatives as corrosion inhibitors for mild steel in hydrochloric acid: experimental and theoretical studies. *J Phys Chem C*. 2015; 119(28):16004-19.
63. Al-Moubaraki AH, Awaji H. 1-X-4-[4'-(OCH₃)-Styryl] pyridinium iodides, potent inhibitors for stainless steel corrosion in 2 M HCl acid solutions. *International J Corr Scale Inhib*. 2020; 9(2):460-501. <https://doi.org/10.17675/2305-6894-2020-9-2-5>.
64. Hoseizadeh AR, Danaee I, Maddahy MH. Thermodynamic and adsorption behaviour of vitamin B1 as a corrosion inhibitor for AISI 4130 steel alloy in HCl solution. *Zeitschrift Für Physikalische Chemie*. 2013; 227(4):403-18.
65. Hammouti B, Zarrouk A, Al-Deyab SS, Warad I. Temperature effect, activation energies and thermodynamics of adsorption of ethyl 2-(4-(2-ethoxy-2-oxoethyl)-2-p-tolylquinoxalin-1 (4H)-yl) acetate on Cu in HNO₃. *Orient J Chem*. 2011; 27(1):23.
66. Amjad Z, Landgraf RT, Penn JL. Calcium sulfate dihydrate (gypsum) scale inhibition by PAA, PAPEMP, and PAA/PAPEMP blend. *Int J Corr Scale Inhib*. 2014; 3(1):35-47. <https://doi.org/10.17675/2305-6894-2014-3-1-035-047>.
67. Valle-Quitana JC, Dominguez-Patiño GF, Gonzalez-Rodriguez JG. Corrosion inhibition of carbon steel in 0.5 M H₂SO₄ by phthalocyanine blue. *Inter Schol Res Not*. 2014; 2014:432-451.
68. Zhao P, Liang Q, Li Y. Electrochemical, SEM/EDS and quantum chemical study of phthalocyanines as corrosion inhibitors for mild steel in 1 mol/l HCl. *Appl Surf Sci*. 2005; 252(5):1596-607. <https://doi.org/10.1016/j.apsusc.2005.02.121>.
69. Sakamoto K, Ohno-Okumura E. Syntheses and functional properties of phthalocyanines. *Materials*. 2009; 2(3):1127-79.
70. De La Torre G, Vázquez P, Agullo-Lopez F, Torres T. Role of structural factors in the nonlinear optical properties of phthalocyanines and related compounds. *Chem Rev*. 2004; 104(9):3723-50. <https://doi.org/10.1021/cr030206t>.
71. García-Sánchez MA, Rojas-González F, Menchaca-Campos EC, Tello-Solís SR, Quiroz-Segoviano RI, Diaz-Alejo LA, Salas-Bañales E, Campero A. Crossed and linked histories of tetrapyrroli-

- cmacrocycles and their use for engineering pores within sol-gel matrices. *Molecules*. 2013; 18(1):588-653.
72. Pesha T, Monama GR, Hato MJ, Maponya TC, Makhatha ME, Ramohlola KE, Molapo KM, Modibane KD, Thomas MS. Inhibition effect of phthalocyaninatocopper (II) and 4-tetranitro (phthalocyaninato) copper (II) inhibitors for protection of aluminium in acidic media. *Inter J Electrochem Sci*. 2019; 14(1):137-49. <https://doi.org/10.20964/2019.01.17>.
 73. Dibetsoe M, Olasunkanmi LO, Fayemi OE, Yesudass S, Ramagathan B, Bahadur I, Adekunle AS, Kabanda MM, Ebenso EE. Some phthalocyanine and naphthalocyanine derivatives as corrosion inhibitors for aluminium in acidic medium: Experimental, quantum chemical calculations, QSAR studies and synergistic effect of iodide ions. *Molecules*. 2015; 20(9):15701-34.
 74. Xu J, Wang Y, Zhang Z. Potential and concentration dependent electrochemical dealloying of Al₂Au in sodium chloride solutions. *J Phys Chem C*. 2012; 116(9):5689-99. <https://doi.org/10.1021/jp210488t>.
 75. Lagrenee M, Mernari B, Bouanis M, Traisnel M, Bentiss F. Study of the mechanism and inhibiting efficiency of 3, 5-bis (4-methylthiophenyl)-4H-1,2,4-triazole on mild steel corrosion in acidic media. *Corr Sci*. 2002; 44(3):573-88. [https://doi.org/10.1016/S0010-938X\(01\)00075-0](https://doi.org/10.1016/S0010-938X(01)00075-0).
 76. Mall ID, Srivastava VC, Agarwal NK, Mishra IM. Adsorptive removal of malachite green dye from aqueous solution by bagasse fly ash and activated carbon-kinetic study and equilibrium isotherm analyses. *Colloid Surf A: Physicochem Eng Aspect*. 2005; 264(1-3):17-28. <https://doi.org/10.1016/j.colsurfa.2005.03.027>.
 77. Noor EA, Al-Moubaraki AH. Thermodynamic study of metal corrosion and inhibitor adsorption processes in mild steel/1-methyl-4 [4'(-X)-styrylpyridinium iodides/hydrochloric acid systems. *Mater Chem Phys*. 2008; 110(1):145-54. <https://doi.org/10.1016/j.matchemphys.2008.01.028>.
 78. Yadav M, Kumar S, Sinha RR, Bahadur I, Ebenso EE. New pyrimidine derivatives as efficient organic inhibitors on mild steel corrosion in acidic medium: electrochemical, SEM, EDX, AFM and DFT studies. *J Mol Liq*. 2015; 211:135-45. <https://doi.org/10.1016/j.molliq.2015.06.063>.
 79. Gao G, Liang C. Electrochemical and DFT studies of β -amino-alcohols as corrosion inhibitors for brass. *Electrochimica Acta*. 2007; 52(13):4554-9. <https://doi.org/10.1016/j.electacta.2006.12.058>.

How to cite this article:

Mohammed A, Betti ZA, Hamood AF, Aljibori HS, Al-Azzawi WK, Kadhum AAAH, Alamiery AA
Guardians Against Corrosion: Exploring Diphenylpyrazoles Through Experimental and DFT
Analysis. *Prog Color Colorants Coat*. 2025;18(1):17-35. <https://doi.org/10.30509/pccc.2024.1672611276>.

